Unified theory of x-ray magnetic circular dichroism at $L_{2,3}$ absorption edges for a series of Ce compounds

A. Kotani*

Photon Factory, Institute of Materials Structure Science, High Energy Accelerator Research Organization, 1-1 Oho, Tsukuba, Ibaraki 305-0801, Japan

(Received 28 July 2008; published 18 November 2008)

A theoretical study is presented with an extended single impurity Anderson model for the spectra of x-ray magnetic circular dichroism (XMCD) at the Ce $L_{2,3}$ edges of mixed-valence Ce compounds under an external magnetic field. The effects of magnetic polariztion of the Ce $4f$ states, the exchange interaction between the Ce $4f$ and $5d$ states, and the hybridization between the Ce $4f$ and ligand states are taken into account. Recent experimental results for $CePd_3$ are well explained. The theory can be applied to the XMCD of a localized Ce^{3+} system, weakly and strongly mixed-valence Ce systems by changing the hybridization strength, and can also be applied to ferromagnetic Ce compounds by replacing the external magnetic field with the ferromagnetic exchange field. The effects of the hybridization in the final state, the Ce $4f^2$ configuration, and the spin polarization of the Ce $5d$ states through the hybridization with a spin-polarized ligand band are studied in detail, and a systematic change in the L_2 and L_3 XMCD intensities with the change in the mixed-valence strength is discussed. The present theory gives a framework to understand varied XMCD behavior of a series of Ce compounds in a unified fashion.

DOI: 10.1103/PhysRevB.78.195115 PACS number(s): 71.20.Eh, 71.20.Lp, 75.20.Hr, 75.30.Mb

I. INTRODUCTION

The Ce $4f$ state of intermetallic Ce compounds changes from a well-localized $4f^1$ state to a mixed-valence state between $4f^0$ and $4f^1$ configurations with the change in the hybridization strength between the $4f$ and conduction electron states.[1–3] Core-level spectroscopy, such as the x-ray absorption spectroscopy (XAS) and its x-ray magnetic circular dichroism (XMCD), is a powerful means to study the electronic states of various Ce compounds.[4,5] In this paper we study theoretically the XAS and XMCD at the $L_{2,3}$ edges of a series of intermetallic Ce compounds.

In Fig. 1(a) we show the change in the Ce $4f$ state (in the ground state) with the change in the hybridization strength or the Kondo temperature T_K which is a measure of the hybridization strength. In the limit of the vanishing hybridization between the $4f$ and conduction electrons, the Ce $4f$ state is well localized, taking the Hund rule ground state of the Ce^{3+} ion. For very weak but finite hybridization strength (with $T_K \sim 10$ K or lower), the Ce $4f$ state is still localized, but the $4f$ magnetic moment is fluctuating due to the hybridization effect (spin-fluctuation regime) and forms a singlet bound state (Kondo state) with the binding energy of $k_B T_K$ [see case (1) of Fig. 1(a)]. Even in this case, if the Ce^{3+} states on the different Ce sites couple ferromagnetically, the ground state can be ordered ferromagnetically instead of taking the singlet state. A typical example is $CeRu_2Ge_2$.

For a weak hybridization strength corresponding to $T_K \sim 100$ K [see case (2) of Fig. 1(a)], a weak charge fluctuation occurs between the Ce $4f$ and conduction electron states. As a result, the system is in the weakly mixed-valence state between the $4f^0$ and $4f^1$ configurations (with a small weight of the $4f^0$ configuration). $CePd_3$ is a typical example. For a strong hybridization strength corresponding to $T_K \sim 1000$ K or higher [see case (3) of Fig. 1(a)], the charge fluctuation is strong and the $4f^0$ and $4f^1$ configurations are mixed strongly with comparable weights. A typical example is $CeFe_2$. It is to be remarked that the Ce $4f$ state in $CeFe_2$ is in the strongly mixed-valence state, but at the same time, the system is in the ferromagnetic state because of the strong exchange interaction between the Fe $3d$ states and the hybridization between the Fe $3d$ and Ce $5d$ states.

The Ce $L_{2,3}$ XAS of Ce compounds is sensitive to the charge fluctuation in the ground state. In the Ce L_2 (L_3) XAS process a $2p_{1/2}$ ($2p_{3/2}$) core electron is excited to the Ce $5d$ band as shown in Fig. 2(a). The experimental Ce L_2 XAS spectra for $CeRu_2Ge_2$, $CePd_3$, and $CeFe_2$ are schematically illustrated in Fig. 1(b). The Ce L_2 XAS spectrum of $CeRu_2Ge_2$ exhibits a single-peak structure corresponding to the well-localized $4f^1$ ground state,[6,7] while that of $CePd_3$ shows a double-peak structure corresponding to the two configurations ($4f^0$ and $4f^1$) mixed in the ground state.[8] For $CePd_3$, the $4f^0$ peak (higher-energy peak) is much weaker in intensity than the $4f^1$ peak (lower-energy peak) and looks similar to a shoulder structure because the weight of the $4f^0$ configuration is much smaller than that of the $4f^1$ configuration in the ground state. $CeFe_2$ also has a double-peak structure in the Ce L_2 XAS, but now the intensities of the two peaks are comparable, reflecting the weights of the $4f^0$ and $4f^1$ configurations in the ground state.[6,7,9] The Ce L_3 XAS spectra of these materials are almost the same as their L_2 XAS spectra, except that the total intensity of the L_3 XAS is twice as large as that of the L_2 XAS due to the degeneracy of the $2p_{3/2}$ and $2p_{1/2}$ core levels.

$CeRu_2Ge_2$ and $CeFe_2$ are ferromagnetic materials where XMCD gives important information on the magnetic character of electronic states especially in the Ce $5d$ state.[5] The experimental result on the L_2 XMCD of $CeRu_2Ge_2$ exhibits a single positive peak with a maximum intensity of about 5% of that of XAS (Refs. 6 and 7) [see Fig. 1(b)]. On the other hand, the L_3 XMCD is much weaker and negative. These results were well explained by Fukui *et al.*,[10] who assumed

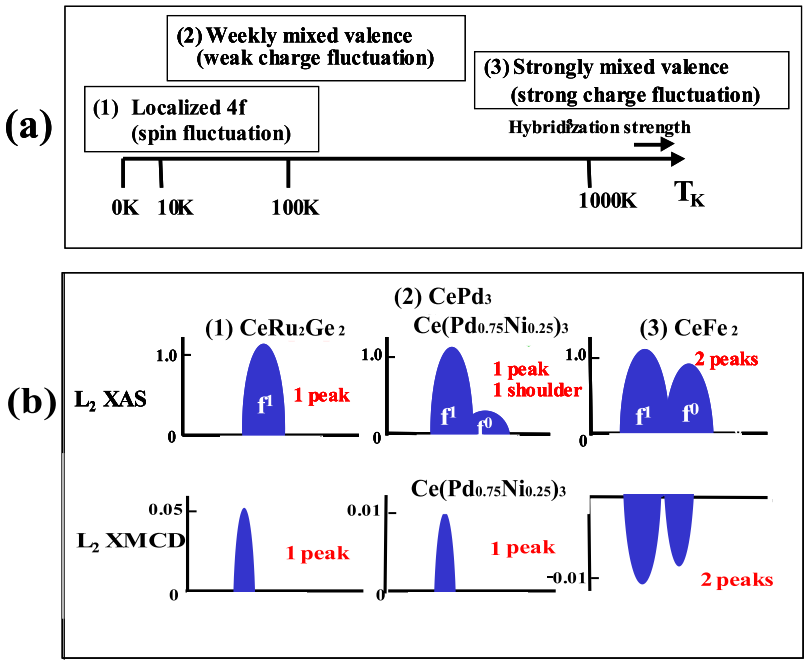

FIG. 1. (Color online) (a) Changes in the Ce $4f$ state with the change in the hybridization strength between Ce $4f$ and conduction band states. (b) Schematic illustration of the spectra of XAS and XMCD at the L_2 edge of various Ce compounds.

that the Ce $4f$ state has no mixed-valence character, and the Ce $5d$ states are magnetically polarized through the exchange interaction with the polarized Ce $4f$ states. The role of the Ce $5d$-$4f$ exchange interaction is to shift the Ce $5d$ energy levels and to enhance the magnitude of the electric dipole transition from the Ce $2p$ to $5d$ states.[11,12] The interaction scheme of electronic states in the theory by Fukui *et al.*[10] is shown in Fig. 2(b).

The experimental Ce $L_{2,3}$ XMCD spectra of $CeFe_2$ have a double-peak structure with the negative (positive) sign at the L_2 (L_3) edge [see Fig. 1(b)]. The XMCD intensity is about 1% of XAS intensity. A theoretical calculation of the Ce $L_{2,3}$ XMCD spectra of $CeFe_2$ was made successfully by Asakura *et al.*[13] with a quite different model from that by Fukui *et al.*[10] Asakura *et al.*[13] assumed that the magnetic polarization of the Ce $4f$ state can be disregarded because of its strong mixed-valence character and that instead the magnetic polarization of the Ce $5d$ state is caused by the hybridization between the Ce $5d$ state and the spin-polarized Fe $3d$ states, as illustrated in Fig. 2(c).

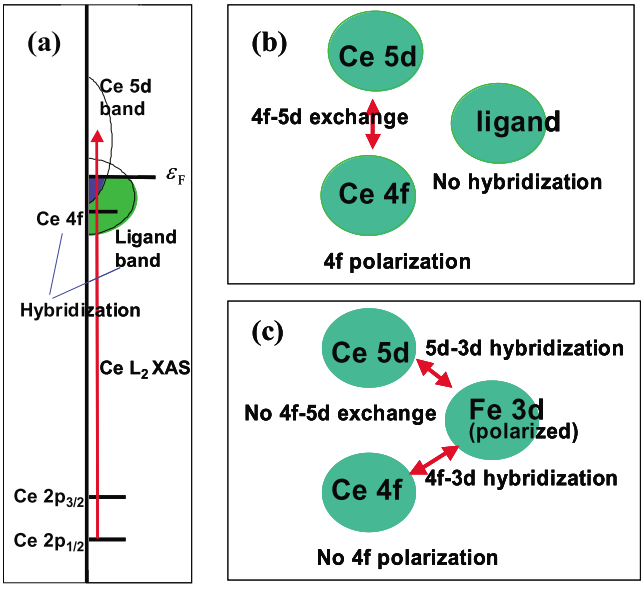

FIG. 2. (Color online) (a) X-ray absorption process at the L_2 edge of Ce compounds. (b) Model of XMCD in $CeRu_2Ge_2$ proposed by Fukui *et al.* (Ref. 10) and (c) that in $CeFe_2$ proposed by Asakura *et al.* (Ref. 13).

Recently experimental observations of the Ce $L_{2,3}$ XMCD were made by Kappler *et al.*[8] for a weakly mixed-valence compound $Ce(Pd_{0.75}Ni_{0.25})_3$, which orders ferromagnetically. The Ce $L_{2,3}$ XAS of $Ce(Pd_{0.75}Ni_{0.25})_3$ is very similar to that of $CePd_3$ with a strong $4f^1$ peak and a weak $4f^0$ peak; but the Ce $L_{2,3}$ XMCD behaves somewhat similarly to that of $CeRu_2Ge_2$ around the $4f^1$ XAS position, whereas no XMCD signal is seen near the $4f^0$ XAS position.[8] The intensity of the L_2 XMCD is about 1% of the XAS intensity as shown in Fig. 1(b), but the intensity of the L_3 XMCD is much weaker with some complicated structure including considerable noises. Furthermore, it was reported by Kappler *et al.*[8] that the XMCD spectra for $CePd_3$ under an external magnetic field of 7 T behave similarly to those of $Ce(Pd_{0.75}Ni_{0.25})_3$ although the XMCD intensity is about one fifth of $Ce(Pd_{0.75}Ni_{0.25})_3$.

It is the purpose of the present paper to explain theoretically the XMCD spectra of $CePd_3$ and $Ce(Pd_{0.75}Ni_{0.25})_3$, especially for the Ce L_2 edge with a single impurity Anderson model (SIAM). To this end, we take into account the mixed-valence character of the Ce $4f$ state as well as the magnetic polarization of the Ce $4f$ state and the exchange interaction between Ce $5d$ and $4f$ states, as shown in Fig. 3(a). Instead of treating the ferromagnetic system, we consider a mixed-valence Ce compound which is magnetized by the external magnetic field; but if we replace the external magnetic field by an exchange field responsible for the ferromagnetic order, the situation will be essentially the same as that in the ferromagnetic systems. The calculated result is in reasonable

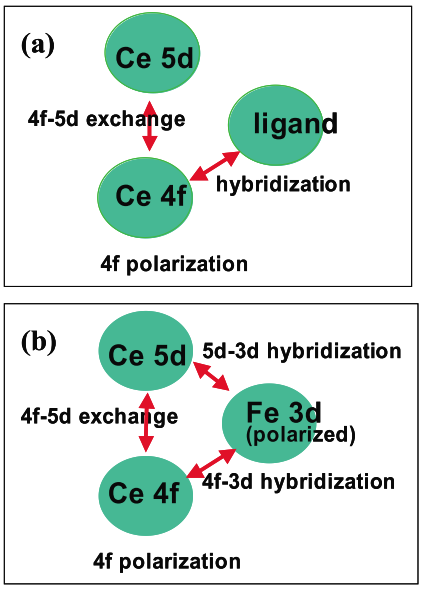

FIG. 3. (Color online) (a) The present model to describe the XMCD of mixed-valence Ce compounds and (b) the model of our unified theory to describe the XMCD for all of $CeRu_2Ge_2$, $CePd_3$, and $CeFe_2$.

agreement with the experimental one. Furthermore, if we change the strength of hybridization between the Ce $4f$ and conduction band states, the theory can also be applied to the localized $4f$ limit (such as $CeRu_2Ge_2$) as well as to the strongly mixed-valence state (such as $CeFe_2$, but the Ce $5d$-Fe $3d$ hybridization is not taken into account within this model). Some results in the initial stage of such calculations have been published as a short paper,[14] where the effects of the final-state hybridization and the $4f^2$ configuration were disregarded for simplicity. In the present paper, these effects are also studied in detail.

Another purpose of the present paper is to propose a unified theory which can be applied to the XMCD calculation of various Ce compound by incorporating the effect of the mixing of the Ce $5d$ state with the spin-polarized band (the Fe $3d$ band for $CeFe_2$) into the theory mentioned above. As shown in Fig. 3(b), here we take into account the magnetic polarization of all the states, Ce $4f$, ligand (Fe) $3d$, Ce $5d$, and all the interactions among them. As mentioned before, the XMCD spectra of $CeRu_2Ge_2$ and $CeFe_2$, respectively, were calculated with quite independent model systems Figs. 2(a) and 2(b) by Fukui *et al.*[10] and Asakura *et al.*[13] However, with the model in Fig. 3(b) we can describe those spectra not only for $CeRu_2Ge_2$ and $CeFe_2$ but also for weakly mixed-valence systems, $CePd_3$ and $Ce(Pd_{0.75}Ni_{0.25})_3$, by changing parameter values included in the model.

The organization of the present paper is as follows. In Sec. II, the formulation of the present theory is given. In Sec. III, we show the dependence of XAS and XMCD on the hybridization strength as a result of numerical calculations. Here the effect of the final-state mixing and the contribution of $4f^2$ configuration are disregarded, but these effects are studied in Sec. IV. In Sec. V the effect of the Ce $5d$ spin polarization due to the hybridization between the Ce $5d$ and the spin-polarized ligand band is combined with the present theory to discuss the XMCD of $CeFe_2$. Section VI is devoted to discussions, and some concluding remarks are given in Sec. VII.

II. FORMULATION

We consider an extended SIAM,[3,15] which consists of the Ce $4f$ and $2p$ states on a single Ce site, the Ce $5d$ band, and the ligand band (which corresponds to the Pd $4d$ band for $CePd_3$). Instead of treating ferromagnetic systems, we consider a mixed-valence Ce compound which is magnetized by an external magnetic field; but if we replace the external magnetic field by an exchange field responsible for the ferromagnetic order, the situation will be essentially the same as that in the ferromagnetic systems. The Hamiltonian of the system is written as

$$H = \sum_{\nu} (\epsilon_{f,\nu} - g_j \mu_B j_z h) f_\nu^\dagger f_\nu + \sum_{\mu} \epsilon_{p,\mu} p_\mu^\dagger p_\mu + \sum_{\xi} \epsilon_{k,\xi} d_{k,\xi}^\dagger d_{k,\xi} + \sum_{k,\nu} \epsilon_k a_{k,\nu}^\dagger a_{k,\nu} + \sum_{k,\nu} (V_k a_{k,\nu}^\dagger f_\nu + V_k^* f_\nu^\dagger a_{k,\nu}) + U_{ff} \sum_{\nu > \nu'} f_\nu^\dagger f_\nu f_{\nu'}^\dagger f_{\nu'} - U_{fc} \sum_{\nu,\mu} f_{f,\nu}^\dagger f_{f,\nu} (1 - p_{p,\mu}^\dagger p_{p,\mu}), \quad (1)$$

where the first, second, third, and fourth terms represent, respectively, the single electron energies of the Ce $4f$ states, the Ce $2p$ states, the Ce $5d$ band, and the ligand band, the fifth term represents the hybridization between Ce $4f$ and ligand band states, the sixth term represents the Coulomb interaction between Ce $4f$ electrons, and the last term is the attractive $2p$ core hole potential acting on the $4f$ state. We disregard the effect of the atomic multiplet coupling which originates from the multipole components of the Coulomb interaction. The external magnetic field is represented by h, and g_j and μ_B are Landé g factor and the Bohr magneton, respectively. The Ce $4f$ and $2p$ states are represented in the JJ coupling scheme and indices ν and μ denote a set of quantum numbers (j, j_z) and (j', j_z') of the $4f$ and $2p$ states, respectively. Therefore, $\epsilon_{f,\nu} = \epsilon_f + (3/7)\delta_f$ (for $j = 7/2$) and $\epsilon_f - (4/7)\delta_f$ (for $j = 5/2$), and $\epsilon_{p,\mu} = \epsilon_p + (1/3)\delta_p$ (for $j' = 3/2$) and $\epsilon_p - (2/3)\delta_p$ (for $j' = 1/2$), where δ_f and δ_p are the spin-orbit splittings of the $4f$ and $2p$ states, respectively. The index k represents the energy levels of the ligand and Ce $5d$ bands; but in the following we disregard the width of the ligand band, for simplicity, and the energy of a single energy level ϵ_k is fixed just at the Fermi level ϵ_F. Except for Sec. V, the width of the Ce $5d$ band is also disregarded, and the energy of $5d$ states ϵ_d is put above the Fermi level. The operators $d_{k,\xi}$ and $a_{k,\nu}$ are written as d_ξ and a_ν, respectively, and the hybridization matrix element V_k is written as V. Also we disregard the effect of the $4f^2$ configurations by putting $U_{ff} = \infty$ (except for Sec. IV B). The calculations are straightforward, extended to the cases of finite values of U_{ff} and the finite width of the $5d$ band, and will be treated in Secs. IV B and V.

The ground state $|g\rangle$ (with energy E_g) is obtained by diagonalizing the Hamiltonian H with 15 basis states (one $4f^0$ state $|0\rangle$ and 14 $4f^1$ states $|j, j_z\rangle$) in the form,

$$|g\rangle = c_0^{(g)}|0\rangle + \sum_{j,j_z} c_{j,j_z}^{(g)}|j,j_z\rangle. \quad (2)$$

Here, we note that $|0\rangle$ is the state where all electrons (except for $4f$ electrons) occupy below ϵ_F and $|j,j_z\rangle = f_{j,j_z}^{\dagger} a_{j,j_z}|0\rangle$.

In the final state, a $2p$ electron is excited to a $5d$ state so that the $4f$ level is pulled down by the core hole potential U_{fc}. We use the LS coupling scheme to describe the Ce $5d$ state by disregarding the spin-orbit interaction with index ξ denoting the combined orbital and spin quantum numbers (m_d, s_d). Then, the final states where a $2p$ electron with $\mu = (j', j_z')$ is excited to the $5d$ state specified by $\xi = (m_d, s_d)$ are described in the following form:

$$|f_{i,\xi,\mu}\rangle = c_0^{(i,\xi,\mu)} d_{\xi}^{\dagger} p_{\mu}|0\rangle + \sum_{j,j_z} c_{j,j_z}^{(i,\xi,\mu)} d_{\xi}^{\dagger} p_{\mu}|j,j_z\rangle, \quad (3)$$

where index i denotes the quantum number of each final state. The energies of the states $d_{\xi}^{\dagger} p_{\mu}|0\rangle$ and $d_{\xi}^{\dagger} p_{\mu}|j,j_z\rangle$ before switching on the hybridization are given by

$$\epsilon_d - \epsilon_{p,\mu} \quad (4)$$

and

$$\epsilon_{\xi} - \epsilon_{p,\mu} + \epsilon_{f,\nu} - U_{fc} - g_j \mu_B j_z h - \epsilon_F, \quad (5)$$

respectively, and these states are coupled through the matrix element of hybridization V. The energy eigenvalue of $|f_{i,\xi,\mu}\rangle$ is written as $E_{i,\xi,\mu}$.

It is important to take into account the exchange interaction energy $E_{\mathrm{ex}}(m_d, s_d; j, j_z)$ between the $5d$ $[\xi = (m_d, s_d)]$ and $4f$ $[\nu = (j, j_z)]$ states given by

$$E_{\mathrm{ex}}(m_d, s_d; j j_z) = \sum_k G^k(4f, 5d) \sum_{q=-k}^{k} \sum_{m_f} \times \left|\left\langle 3m_f \tfrac{1}{2} s_d | j j_z \right\rangle\right|^2 |c^k(2m_d, 3m_f)|^2, \quad (6)$$

where $G^k(4f, 5d)$ is the $4f$-$5d$ Slater integrals, $\langle j_1 m_1 j_2 m_2 | j j_z \rangle$ is the Wigner coefficient, and c^k is proportional to the Clebsch-Gordan coefficient. Therefore, the energy ϵ_{ξ} in Eq. (5) is replaced by

$$\epsilon_{\xi} = \epsilon_d + E_{\mathrm{ex}}(m_d, s_d; j, j_z). \quad (7)$$

This type of exchange-induced energy shift of the Ce $5d$ state was first introduced by Jo and Imada[16] in their theory of XMCD and used by Matsuyama *et al.*[11] to develop further the theory by introducing the enhancement effect of the electric dipole transition intensity.[17]

The matrix element of the electric dipole transition from the $2p_{j', j_z'}$ to $5d_{m_d, s_d}$ states by $\pm$ helicity light is represented by

$$M^{\pm}(m_d, s_d; j', j_z') = \sum_{m_p} \langle 1 m_p 1 \pm 1 | 2 m_d \rangle \left\langle 1 m_p \tfrac{1}{2} s_d | j' j_z' \right\rangle. \quad (8)$$

As pointed out by Matsuyama *et al.*,[11] it is essential to renormalize $M^{\pm}$ into $\tilde{M}^{\pm}$ by taking into account the enhancement effect of the transition intensity by the exchange interaction,

$$\tilde{M}^{\pm}(j, j_z; m_d, s_d; j', j_z') = M^{\pm}(m_d, s_d; j', j_z') \times [1 - \alpha E_{\mathrm{ex}}(m_d, s_d; j, j_z)]^{1/2}, \quad (9)$$

where the Ce $4f$ state is assumed to be in (j, j_z).[18] Then the matrix element, $\langle f_{i,\xi,\mu}|\tilde{M}^{\pm}|g\rangle$, of the renormalized dipole transition operator from the ground state $|g\rangle$ to each final state $|f_{i,\xi,\mu}\rangle$ is given by

$$\langle f_{i,\xi,\mu}|\tilde{M}^{\pm}|g\rangle = M^{\pm}(\xi;\mu)\left\{ c_0^{(i,\xi,\mu)*} c_0^{(g)} + \sum_{j,j_z} c_{j,j_z}^{(i,\xi,\mu)*} c_{j,j_z}^{(g)} \times [1 - \alpha E_{\mathrm{ex}}(\xi; j, j_z)]^{1/2} \right\}. \quad (10)$$

The L_2 and L_3 XAS spectra for $\pm$ helicity light is expressed as

$$F_{j'}^{\pm}(\omega) = \sum_{\xi,i,j_z'} |\langle f_{i,\xi,\mu}|\tilde{M}^{\pm}|g\rangle|^2 \frac{\frac{\Gamma}{\pi}}{(\omega - E_{i,\xi,\mu} + E_g)^2 + \Gamma^2}, \quad (11)$$

where ω is the incident x-ray energy, Γ is the spectral broadening due to the lifetime of the $2p$ core hole, and $j' = 1/2$ and $3/2$ for the L_2 and L_3 XAS, respectively. If we disregard the hybridization V in the final state, the formulation given here reduces to that in Ref. 14.

III. DEPENDENCE OF X-RAY ABSORPTION AND X-RAY MAGNETIC CIRCULAR DICHROISM SPECTRA ON THE HYBRIDIZATION STRENGTH

We study the dependence of XAS and XMCD spectra on the strength of hybridization between the Ce $4f$ and the ligand band. In this section we disregard, for simplicity, the hybridization effect in the final state and assume that each of the Ce $5d$ and ligand bands is a single level, neglecting the band width. Numerical calculations of XAS $(F_{j'}^{+} + F_{j'}^{-})$ and XMCD $(F_{j'}^{+} - F_{j'}^{-})$ are made using the parameter values, $\epsilon_f - \epsilon_F = -1.0$ eV, $U_{fc} = 10.5$ eV, $\alpha = 0.6$ eV^{-1}, $\Gamma = 3.0$ eV, and $G^1(4f, 5d) = 1.0$ eV (by disregarding G^3 and G^5). The strength of the external magnetic field is taken as $\epsilon_H = g\mu_B h = 0.001$ eV with the g factor of a single electron spin $(g = 2.0023)$, which corresponds to the external field strength $h = 8.69$ T. The present description of the external field strength is more convenient than $\tilde{h} = g_j \mu_B h$ (with the Landé g-factor g_j) in Ref. 14. The hybridization strength V in the ground state (denoted by V_g) is changed as a parameter. All calculations in this paper are made at zero temperature.

A. Localized Ce^{3+} state

First we put $V_g = 0.0001$ eV, where the hybridization is extremely small. In this case the ground state is given by the almost pure Ce^{3+} (trivalence) state with $|c_{5/2,5/2}^{(g)}|^2 \cong 1.0$ and with almost vanishing $|c_0^{(g)}|^2$ and $|c_{j,j_z}^{(g)}|^2$ for $(j, j_z) \neq (5/2, 5/2)$. Since we disregard the final-state hybridization, the final states are given by $d_{\xi}^{\dagger} p_{\mu}|0\rangle$ and $d_{\xi}^{\dagger} p_{\mu}|j, j_z\rangle$; but the states contributing to the XAS and XMCD are only

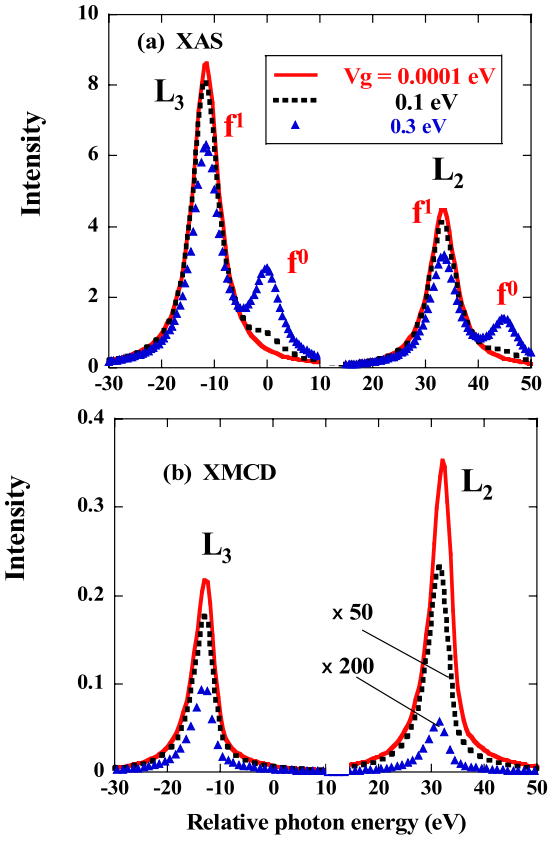

FIG. 4. (Color online) (a) XAS and (b) XMCD spectra calculated for a localized Ce^{3+} state (V_g=0.0001 eV), weakly mixed-valence (V_g=0.1 eV), and strongly mixed-valence (V_g=0.3 eV) states.

$d^{\dagger}_{\xi}p_{\mu}|5/2,5/2\rangle$ because the transition matrix element $M^{\pm}(m_d,s_d;j',j'_z)$ [Eq. (8)] connects only the $2p(j',j'_z)$ and $5d(m_d,s_d)$ states and the weight of the final state $|i\rangle$ (=$|0\rangle$ and $|j,j_z\rangle$) is given by the overlap integral $|\langle g|i\rangle|^2=|c_i^{(g)}|^2$. Therefore, the XAS and XMCD spectra are given by those of the atomic Ce^{3+} state. The calculated results are shown in Fig. 4(a) for XAS and in Fig. 4(b) for XMCD. It is seen that the XAS and XMCD spectra for each of the L_2 and L_3 edges exhibit a single-peak structure. The ratio of integrated intensities of XMCD and XAS ($I_{\mathrm{XMCD}}/I_{\mathrm{XAS}}$) is 0.0636 for L_2 edge and 0.0206 for L_3 edge. These values are consistent with those obtained by Matsuyama *et al.*[11] although they treated the $4f$ states by the *LS* scheme instead of the present *JJ* scheme.

B. Weakly mixed-valence state

Here, we take the initial-state hybridization V_g=0.1 eV, which corresponds to that of weakly mixed-valence systems such as $CePd_3$. By diagonalizing the Hamiltonian, the weights in the ground state are given by $|c_0^{(g)}|^2$=0.0592, $|c^{(g)}_{5/2,5/2}|^2$=0.153, $|c^{(g)}_{5/2,3/2}|^2$=0.151, $|c^{(g)}_{5/2,1/2}|^2$=0.149, $|c^{(g)}_{5/2,-1/2}|^2$=0.147, $|c^{(g)}_{5/2,-3/2}|^2$=0.145, and $|c^{(g)}_{5/2,-5/2}|^2$=0.143, and the weight of j=7/2 is much smaller (about 0.05 in total). The calculated XAS and XMCD spectra are shown with solid squares in Figs. 4(a) and 4(b), respectively. It is to be noted that the intensity of XMCD is enlarged 50 times in Fig. 4(b). Each of L_2 and L_3 XAS spectra has a double-peak structure (a peak and a shoulder), and the integrated intensity ratio is given by $1-|c_0^{(g)}|^2:|c_0^{(g)}|^2=0.941:0.059$ because they correspond to the weights of the $4f^1$ and $4f^0$ configurations, respectively. On the other hand, each of L_2 and L_3 XMCD spectra exhibits a single peak at the position of the $4f^1$ configuration. This is because the $5d$ final states corresponding to the $4f^0$ configuration have no exchange potential, and thus there are no exchange energy shift and no enhancement effect of the transition intensity. The values of $I_{\mathrm{XMCD}}/I_{\mathrm{XAS}}$ is 0.000 871 for L_2 and 0.000 337 for L_3. The fact that $I_{\mathrm{XMCD}}/I_{\mathrm{XAS}}$ is larger for L_2 than for L_3 and that the value of $I_{\mathrm{XMCD}}/I_{\mathrm{XAS}}$ for L_2 is of the order of 10^{-3} are in agreement with experimental results of $CePd_3$ at 7 T. The reason why $I_{\mathrm{XMCD}}/I_{\mathrm{XAS}}$ of mixed-valence systems is much smaller than that of the Ce^{3+} is understood easily. In the case of Ce^{3+} the final state $|5/2,5/2\rangle$ has a 100% weight and contributes to the XMCD; but in the present mixed-valence case the final state $|5/2,5/2\rangle$ has only a 15.3% weight. Furthermore, the contribution from the $|5/2,5/2\rangle$ final state to XMCD is opposite to that from the $|5/2,-5/2\rangle$ final state so that most of the 15.4% weight is canceled out and only the difference of the two weights, 15.3%−14.3%=1.0%, gives the net contribution to XMCD. Thus, the present mixed-valence system gives the XMCD intensity only about 1.0% of the Ce^{3+} systems. Some more discussions on this point, as well as the contribution from j=7/2 states, will be given in Sec. VI.

C. Strongly mixed-valence state

We take V_g=0.3 eV, corresponding to strongly mixed-valence systems such as $CeFe_2$. In this case, the ground-state weights are $|c_0^{(g)}|^2$=0.287, and all of j=5/2(7/2) states are around 0.07 (0.035): for instance, $|c^{(g)}_{5/2,5/2}|^2$=0.0716, $|c^{(g)}_{5/2,-5/2}|^2$=0.0711, $|c^{(g)}_{7/2,7/2}|^2$=0.0357, $|c^{(g)}_{7/2,-7/2}|^2$=0.0354, and so on. Therefore, the XAS spectra have a double-peak structure with an intensity ratio 0.713: 0.287, as seen from the calculated results shown by triangles in Fig. 4(a). The calculated XMCD spectra are shown by triangles in Fig. 4(b) with the intensity 200 times enlarged. The present XMCD intensity is found to be much weaker than that of the weakly mixed-valence systems. From the consideration similar to that made for the weakly mixed-valence systems, the XMCD intensity of the present strongly mixed-valence system is about 0.05% that of the Ce^{3+} system. The present XMCD intensity is 1 order of magnitude smaller than that of the preceding weakly mixed-valence system.

It is interesting to consider the branching ratio of the XMCD intensities for L_2 and L_3 edges. The calculated results in Fig. 4(b) show that the XMCD intensity at the L_2 edge is larger than that at the L_3 edge for the cases of localized Ce^{3+} and weakly mixed-valence systems, but it is smaller at the L_2 edge than at the L_3 edge for the strongly mixed-valence system. This will be discussed in Sec. VI.

D. Comparison with experimental results

The present calculations explain considerably well the experimental results for $CePd_3$ as mentioned before. Further-

more, we can discuss the experimental results for ferromagnetic systems by replacing the external magnetic field by the ferromagnetic exchange field. In the case of Ce^{3+} systems, the local magnetic moment is saturated at zero temperature (or at low temperatures) so that the effect of the external field on XMCD is the same as that of the exchange field. The present result is consistent with the experimental data of $CeRu_2Ge_2$ at the L_2 edge. As shown by Fukui *et al.*,[10] reproducing the experimental result at the L_3 edge would require taking into account the effect of the crystal field, which is disregarded in the present calculation. The calculated result for the weakly mixed-valence system is similar, especially for the L_2 edge, to the experimental data of $Ce(Pd_{0.75}Ni_{0.25})_3$; but the calculated XMCD intensity is smaller than the experimental one. This can be explained by the fact that the ferromagnetic exchange field is stronger than the external field strength taken in the present calculation. For the L_3 edge of $CePd_3$ and $Ce(Pd_{0.75}Ni_{0.25})_3$, the experimental XMCD intensity is much smaller than the calculated one and furthermore seems to have some complicated structures although the signal-to-noise ratio is low. In order to discuss these XMCD spectra at the L_3 edge, more quantitative theoretical calculations, as well as more precise experimental measurements, would be necessary.

The XMCD intensity calculated for the strongly mixed-valence system is much smaller than the experimental result for $CeFe_2$. In order to explain the experimental result, it is necessary to take into account the spin polarization of the Ce $5d$ states due to the hybridization between Ce $5d$ and Fe $3d$ states, as shown by Asakura *et al.*[13] The calculation of XMCD will be given in Sec. V by taking into account both the magnetization of the Ce $4f$ state and the Ce $5d$ spin polarization originating from this hybridization effect.

IV. EFFECTS OF FINAL-STATE MIXING AND THE CONTRIBUTION FROM $4f^2$ CONFIGURATION

A. Final-state mixing

We study the effect of the hybridization in the final state for the two cases treated in Secs. III B and III C. First we consider the weakly mixed-valence system with the initial-state hybridization V_g=0.1 eV and calculate XAS and XMCD spectra by switching on the final-state hybridization V_f. The calculated XAS and XMCD spectra are depicted in Figs. 5(a) and 5(b), respectively, where the results with V_f =0.1 and 0.0 eV are shown with curve and solid circles, respectively. It is seen that the results with and without the final-state mixing almost coincide with each other for both XAS and XMCD spectra so that the effect of the final-state mixing can be neglected. This justifies our assumption of disregarding the final-state mixing for the case of V_g =0.1 eV in the preceding section.

Next we consider the strongly mixed-valence system with V_g=0.3 eV. Figures 6(a) and 6(b) are, respectively, the calculated XAS and XMCD spectra where curve and solid circles are obtained for V_f=0.3 and 0.0 eV, respectively. It is seen that the XAS spectrum depends to some extent on the final-state mixing, and a part of the oscillator strength of the

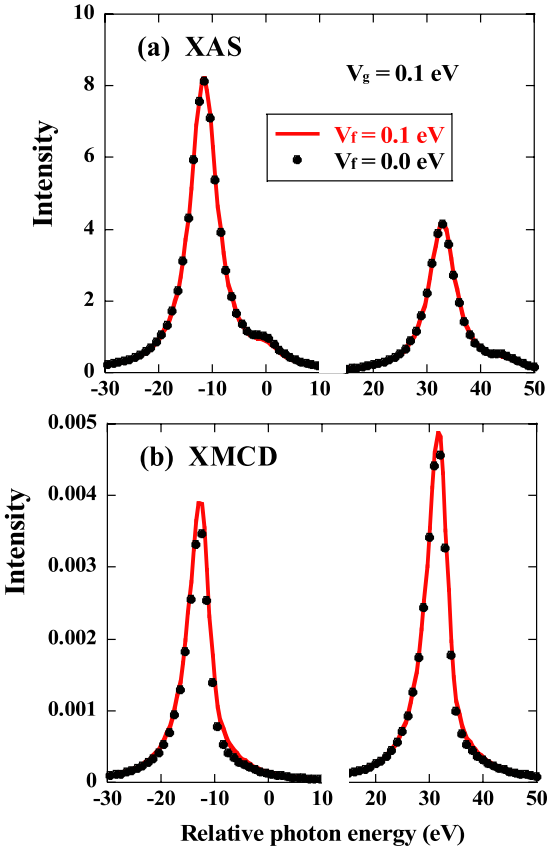

FIG. 5. (Color online) (a) XAS and (b) XMCD spectra calculated for the initial-state hybridization V_g=0.1 eV with (V_f =0.1 eV) and without (V_f=0.0 eV) the final-state hybridization.

$4f^0$ peak transfers to the $4f^1$ peak. On the other hand, the XMCD spectrum is almost independent of the final-state hybridization. If we look at Fig. 6(b) carefully, the XMCD intensity at the $4f^0$ energy position is slightly smaller for V_f=0.3 eV than for V_f=0.0 eV, and this part is shown in the inset with extended scale. This is the effect of the final-state mixing; the final states at the $4f^0$ energy position include a small amount of (j,j_z) components which give a weak negative contribution to the XMCD.

The present results indicate that in the case of V_g =0.3 eV our assumption of disregarding the final-state hybridization is justified for XMCD and acceptable as an approximate treatment for XAS.

B. Contribution from $4f^2$ configuration

The effect of the $4f^2$ configuration on the XAS and XMCD spectra is studied for the weakly mixed-valence case with V_g=V_f=0.1 eV. In order to make the calculation tractable, we approximately confine ourselves to the Ce $4f$ states with j=5/2. The ground state is now expressed as

$$|g\rangle = c_0^{(g)}|0\rangle + \sum_{j_z} c_{j,j_z}^{(g)}|j,j_z\rangle + \sum_{j_{1z}\neq j_{2z}} c_{j,j_{1z},j_{2z}}^{(g)}|j,j_{1z},j_{2z}\rangle, \tag{12}$$

and each final state is written as

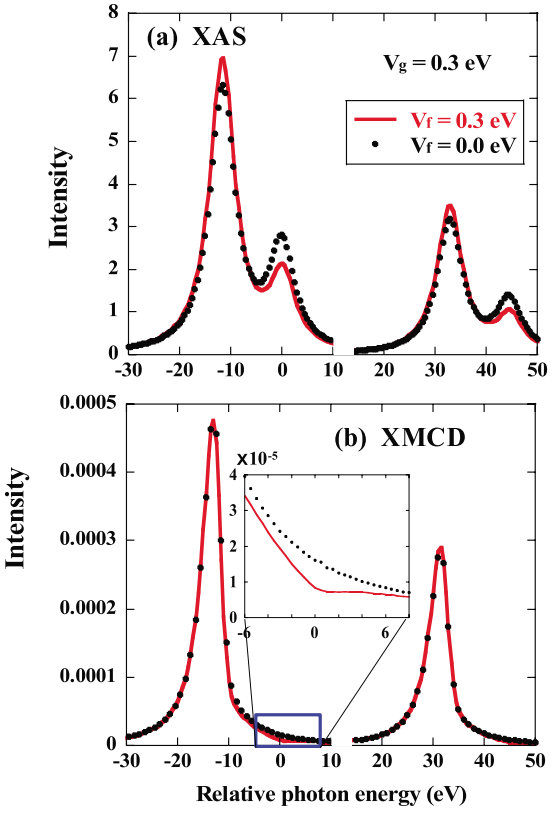

FIG. 6. (Color online) (a) XAS and (b) XMCD spectra calculated for the initial-state hybridization V_g=0.3 eV with (V_f =0.3 eV) and without (V_f=0.0 eV) the final-state hybridization.

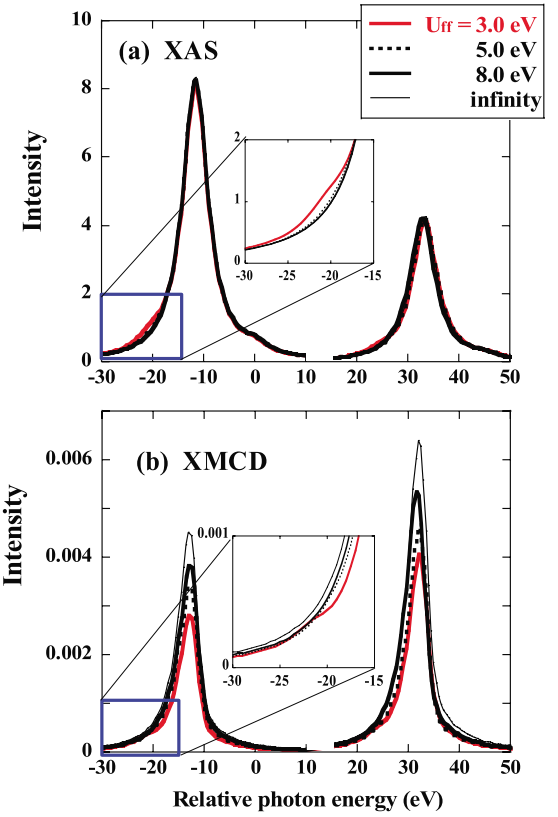

FIG. 7. (Color online) (a) XAS and (b) XMCD spectra calculated for the hybridization strength V_g=V_f=0.1 eV by changing the Coulomb interaction strength U_{ff}.

$$|f_{i,\xi,\mu}\rangle = c_0^{(i,\xi,\mu)} d_\xi^\dagger p_\mu |0\rangle + \sum_{j_z} c_{j,j_z}^{(i,\xi,\mu)} d_\xi^\dagger p_\mu |j,j_z\rangle + \sum_{j_{1z} \neq j_{2z}} c_{j,j_{1z},j_{2z}}^{(i,\xi,\mu)} d_\xi^\dagger p_\mu |j,j_{1z},j_{2z}\rangle, \quad (13)$$

where j is fixed at 5/2, and $|j,j_{1z},j_{2z}\rangle$ is defined by

$$|j,j_{1z},j_{2z}\rangle = f_{j,j_{1z}}^\dagger a_{j,j_{1z}} f_{j,j_{2z}}^\dagger a_{j,j_{2z}} |0\rangle. \quad (14)$$

We also take into account the exchange interaction energy $E_{\rm ex}(m_d,s_d;j,j_{1z},j_{2z})$ between 5d and 4f states when the 4f state is in the $4f^2$ configuration with (j,j_{1z}) and (j,j_{2z}) in the following form:

$$E_{\rm ex}(m_d,s_d;j,j_{1z},j_{2z}) = E_{\rm ex}(m_d,s_d;j,j_{1z}) + E_{\rm ex}(m_d,s_d;j,j_{2z}). \quad (15)$$

The calculated results for the XAS and XMCD spectra are shown in Figs. 7(a) and 7(b), respectively. The value of U_{ff} is taken to be 3.0 eV, 5.0 eV, 8.0 eV, and ∞. For U_{ff} =3.0 eV, the XAS and XMCD spectra exhibit an extra structure on the lower-energy side of the main peak ($4f^1$ peak), corresponding to the energy position of the $4f^2$ configuration [see the insets of Figs. 7(a) and 7(b)]. This structure disappears for other values of U_{ff}. The XAS spectra for U_{ff} =5.0 eV, 8.0 eV, and ∞ almost coincide with each other, but the XMCD intensity of the main peak increases with U_{ff}. For many mixed-valence Ce compounds, the value of U_{ff} has been estimated to be 6.0$\sim$8.0 eV.[3,13,15] If we compare the results for U_{ff}=8.0 eV and ∞, it is seen that the effect of the $4f^2$ configuration is fully negligible for XAS and almost negligible for XMCD.

Here we have disregarded the effect of the j=7/2 states; but from the comparison of the results for U_{ff}=∞ in Fig. 7 and for V_g=V_f=0.1 eV in Fig. 5, the effect of the j=7/2 states is negligibly small for XAS and results in slightly decreasing the intensity of XMCD. If the value of V_g increases (decreases), the contribution from the j=7/2 states increases (decreases), and this contribution causes the change in the branching ratio of XMCD at L_2 and L_3 edges. We will discuss this effect in more detail in Sec. VI.

V. EFFECT OF 5d SPIN POLARIZATION DUE TO THE HYBRIDIZATION BETWEEN THE Ce 5d AND LIGAND BAND

In describing the XMCD of $CeFe_2$, it is important to take into account the spin polarization of the Ce 5d band due to the hybridization between the Ce 5d band and the spin-polarized Fe 3d band, as shown by Asakura *et al.*[13] Here we incorporate this effect in our calculation made in Sec. III C. We treat the Ce 5d states as energy bands with a width of $2W$=6 eV and assume, following Jo and Imada[16] and Matsuyama *et al.*,[11] that the density of states of each Ce 5$d(d\mu)$ band is given by

$$\rho_{d\mu}(\epsilon) = \left(\frac{2}{\pi W^2}\right)\sqrt{W^2 - (\epsilon - \tilde{E}_{d\mu})^2}, \tag{16}$$

where the center of the $5d(d\mu)$ band, $\tilde{E}_{d\mu}$, is to be determined in the following.

We consider both $j=5/2$ and $7/2$ states and take $V_g=0.3$ eV, disregarding the final-state mixing V_f and the contribution from the $4f^2$ configuration. The ground state is given by Eq. (2), except for the Ce $5d$ states. Then the atomic $5d(d\mu)$ energy level is given, including the exchange interaction with Ce $4f$ states, by

$$E_{d\mu} = \epsilon_d + \sum_{j,j_z} E_{\rm ex}(m_d, s_d; j, j_z)|c^{(g)}_{j,j_z}|^2. \tag{17}$$

Furthermore, we take into account the spin splitting, $D_{\rm spin}$, of the Ce $5d$ states due to the hybridization with the spin-polarized Fe $3d$ band so that $E_{d\mu}$ in the above equation is modified to

$$\tilde{E}_{d\mu} = E_{d\mu} + \left(\frac{D_{\rm spin}}{2}\right)\delta\left(m_d, \frac{1}{2}\right) - \left(\frac{D_{\rm spin}}{2}\right)\delta\left(m_d, -\frac{1}{2}\right), \tag{18}$$

where $\delta(m_d, \pm 1/2)$ is the Kronecker delta function. This $\tilde{E}_{d\mu}$ is taken to be the center of each Ce $5d(d\mu)$ band. The Fermi energy ϵ_F is determined by assuming that the total $5d$ electron number (per Ce atom) is unity so that

$$\sum_{m_d, s_d} \int_{-\infty}^{\epsilon_F} \rho_{d\mu}(\epsilon) d\epsilon = 1. \tag{19}$$

Since we assume $V_f=0$, the final states are $d^\dagger_\xi p_\mu|0\rangle$ and $d^\dagger_\xi p_\mu|j, j_z\rangle$, apart from the $5d(d\mu)$ band electron states which exist originally in the ground state. On going from the ground state to each final state, each $5d(d\mu)$ band changes in energy because the exchange energy changes from $\Sigma_{j,j_z} E_{\rm ex}(m_d, s_d; j, j_z)|c^{(g)}_{j,j_z}|^2$ to 0 (for $d^\dagger_\xi p_\mu|0\rangle$) and $E_{\rm ex}(m_d, s_d; j, j_z)$ (for $d^\dagger_\xi p_\mu|j, j_z\rangle$). However, any rearrangements of electron population among $5d(d\mu)$ bands should not occur because if any rearrangements occur, the overlap integral of the $5d$ band states between the ground and the final states vanishes in the present model. Therefore, the calculations of XAS and XMCD spectra are straightforward by fixing the $5d(d\mu)$ electron population and by calculating the $2p$-$5d$ dipole transition only for the empty states of each $5d(d\mu)$ band.

The calculated XAS and XMCD spectra are shown for various values of $D_{\rm spin}$ in Figs. 8(a) and 8(b), respectively. The XAS spectrum is almost independent of $D_{\rm spin}$, and a small deviation from the result for $V_g=0.3$ eV in Fig. 4(a) is due to the effect of the finite width of the Ce $5d$ band. On the other hand, the XMCD spectrum depends strongly on the value of $D_{\rm spin}$. In the case of $D_{\rm spin}=0.0$ eV, the result is essentially the same as that in Fig. 4(b). With increasing $D_{\rm spin}$, the XMCD spectrum has additional contribution of positive double peaks for the L_3 edge and negative double peaks for the L_2 edge. In the case of $D_{\rm spin}=0.3$ eV, the amplitude of the XMCD is of the order of 1.0% of the XAS amplitude, in agreement with the experimental result of

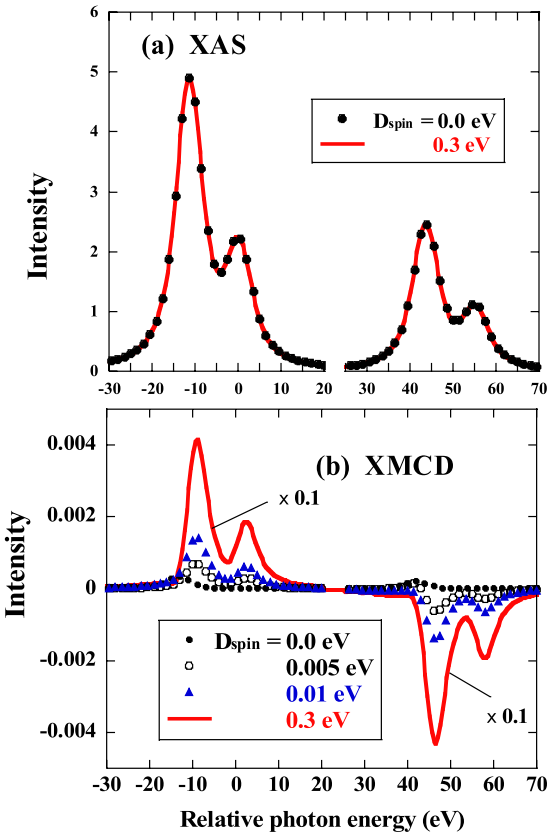

FIG. 8. (Color online) (a) XAS and (b) XMCD spectra calculated for the hybridization strength $V_g=0.3$ eV ($V_f=0.0$ eV) and by changing the spin splitting of the Ce $5d$ band, $D_{\rm spin}$, due to the hybridization with the spin-polarized ligand band.

$CeFe_2$. In this case the XMCD amplitude (mainly originating from $D_{\rm spin}$) is about 100 times as large as that originating from the magnetic polarization of the Ce $4f$ state (i.e., in the case of $D_{\rm spin}=0.0$ eV). The present result confirms explicitly the assumption by Asakura *et al.* that the magnetic polarization of the Ce $4f$ state can be disregarded in the calculation of the XMCD for $CeFe_2$.

VI. DISCUSSION

An interesting finding in the present paper is that the branching ratio $I_{\rm XMCD}(L_2)/I_{\rm XMCD}(L_3)$ changes systematically with the change in V_g. Here we discuss the reason for this in some detail, assuming $V_f=0$. The eigenfunctions of Ce $4f$ and ligand states in the final state of XAS are given by $|0\rangle$ and $|j, j_z\rangle$, where $|0\rangle$ does not contribute to XMCD. Therefore, we can decompose the XMCD spectra at the L_2 and L_3 edges into the contribution from each $|j, j_z\rangle$ state in the following form:

$$F^+_{j'}(\omega) - F^-_{j'}(\omega) = \sum_{j,j_z} f_{j',j,j_z}(\omega)|c^{(g)}_{j,j_z}|^2, \tag{20}$$

where f_{j',j,j_z} is expressed as

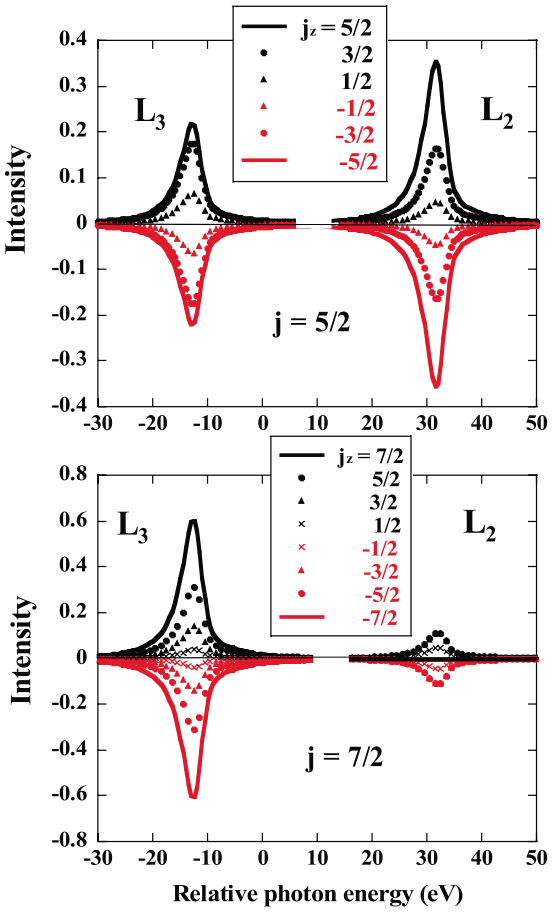

FIG. 9. (Color online) The behavior of $f_{j',j,j_z}(\omega)$ as a function of the relative photon energy ω for various values of j_z and for $j=5/2$ (upper panel) and 7/2 (lower panel). For the definition of $f_{j',j,j_z}(\omega)$, see the text.

$$f_{j',j,j_z}(\omega) = \sum_{m_d,s_d,j'_z} \left(\left| \sum_{m_p} \langle 2m_d 1+1 | 1m_p \rangle \left\langle 1m_p \frac{1}{2} s_d | j' j'_z \right\rangle \right|^2 - \left| \sum_{m_p} \langle 2m_d 1-1 | 1m_p \rangle \left\langle 1m_p \frac{1}{2} s_d | j' j'_z \right\rangle \right|^2 \right) \times [1 - \alpha E_{\mathrm{ex}}(m_d, s_d; j, j_z)] \frac{\frac{\Gamma}{\pi}}{(\omega - E_{j,j_z,\xi,\mu} + E_g)^2 + \Gamma^2}, \tag{21}$$

as easily seen from Eqs. (8)–(11). Here, the final-state energy $E_{j,j_z,\xi,\mu}$ is given by Eq. (5) together with Eq. (7). We remark that each of $f_{j',j,j_z}(\omega)$ is the XMCD spectrum by fixing the final state at $|j,j_z\rangle$ so that it does not include the mixed-valence character of the ground state.[19] On the other hand, the factor $|c^{(g)}_{j,j_z}|^2$ in Eq. (20) reflects the character of the ground state because the contribution from each final state is determined by the overlap integral $|c^{(g)}_{j,j_z}|^2$ between the ground and final states.

The behavior of $f_{j',j,j_z}(\omega)$ is shown in Fig. 9 for each set of values (j,j_z) and for $j'=1/2(L_2)$ and $3/2(L_3)$. It is seen

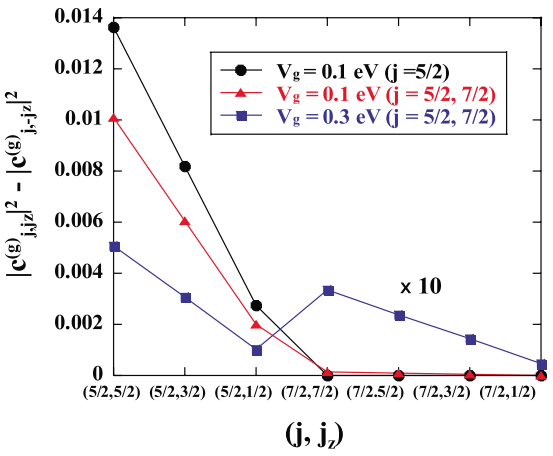

FIG. 10. (Color online) The weight $|c^{(g)}_{j,j_z}|^2 - |c^{(g)}_{j,-j_z}|^2$ plotted as a function of (j,j_z) for different values of the ground-state hybridization strengths, where $|c^{(g)}_{j,j_z}|^2$ is the weight of the basis state (j,j_z) in the ground state.

that $f_{j',j,j_z}(\omega)$ depends strongly on j and j_z. For instance, for $(j,j_z)=(5/2,\pm 5/2)$, the intensity of $f_{j',j,j_z}(\omega)$ at the L_2 edge is about 1.5 times as large as that at the L_3 edge, while for $(j,j_z)=(7/2,\pm 7/2)$, on the contrary, that at the L_3 edge is quite dominant over the L_2 edge and actually the intensity at the L_3 edge is about three times as large as that of $(j,j_z)=(5/2,\pm 5/2)$ and the intensity at the L_2 edge is exactly zero. This behavior is determined only by the selection rule of the $2p$-$5d$ electric dipole transition and the exchange enhancement of this transition intensity and independent of the mixed-valence character of the ground state. Combining $f_{j',j,j_z}(\omega)$ with the ground-state character $|c^{(g)}_{j,j_z}|^2$, we can learn many things as shown below.

As $f_{j',j,j_z}(\omega)$ satisfies the relation,

$$f_{j',j,j_z}(\omega) = -f_{j',j,-j_z}(\omega), \tag{22}$$

we can rewrite the XMCD spectrum as

$$F^+_{j'}(\omega) - F^-_{j'}(\omega) = \sum_{j,j_z(>0)} f_{j',j,j_z}(\omega)[|c^{(g)}_{j,j_z}|^2 - |c^{(g)}_{j,-j_z}|^2]. \tag{23}$$

For instance, for the localized Ce^{3+} system, $|c^{(g)}_{j,j_z}|^2$ does not vanish only for $|c^{(g)}_{5/2,5/2}|^2$ (=1.0) so that the XMCD spectrum is simply given by $f_{j',j,j_z}(\omega)$ for $(j,j_z)=(5/2,5/2)$ in Fig. 9 (compare this with the corresponding curve in Fig. 4). It is seen that the XMCD intensity at the L_2 edge is 1.59 times as large as that at the L_3 edge. For mixed-valence systems with $V_g=0.1$ and 0.3 eV, the value of $|c^{(g)}_{j,j_z}|^2 - |c^{(g)}_{j,-j_z}|^2$ is shown in Fig. 10 for each combined value of (j,j_z). For $V_g=0.1$ eV, the calculation is made in the two cases where we take into account (1) both $j=5/2$ and 7/2 and (2) only $j=5/2$, but first we consider the case (1). Here the most dominant contribution of $|c^{(g)}_{j,j_z}|^2 - |c^{(g)}_{j,-j_z}|^2$ (=0.01) comes from $(j,j_z)=(5/2,5/2)$ so that the rough estimation of XMCD is about 1.0% of the Ce^{3+} system, as mentioned in Sec. III B. More quantitatively, however, the next dominant contribution from $(j,j_z)=(5/2,3/2)$ gives a considerable correction (the correction is about 50% for L_3 and about 25% for L_2 with re-

spect to the most dominant value). As seen from Fig. 9, the intensity of $f_{j',j,j_z}(\omega)$ for $(j,j_z)=(5/2,3/2)$ is slightly larger at L_3 than at L_2 so that the branching ratio $I_{\mathrm{XMCD}}(L_2)/I_{\mathrm{XMCD}}(L_3)$ for $V_g=0.1$ eV becomes 1.31, which is smaller than that for the localized Ce^{3+} system. For the strongly mixed-valence system with $V_g=0.3$ eV, $|c^{(g)}_{j,j_z}|^2 - |c^{(g)}_{j,-j_z}|^2$ from $(j,j_z)=(5/2,5/2)$, (5/2,3/2), and (7/2,7/2) give considerable contributions to the XMCD intensity. In determining the branching ratio $I_{\mathrm{XMCD}}(L_2)/I_{\mathrm{XMCD}}(L_3)$, the contribution from $(j,j_z)=(7/2,7/2)$ plays the most important role. Moreover as a result the branching ratio becomes about 0.59, in sharp contrast to those for $V_g=0.0001$ and 0.1 eV.

Let us consider the case of $V_g=0.1$ eV, taking into account only $j=5/2$ states. As seen in Fig. 10, the direct contribution from the $j=7/2$ states to the XMCD spectrum is negligibly small, but the calculated results of $|c^{(g)}_{j,j_z}|^2-|c^{(g)}_{j,-j_z}|^2$ for $j=5/2$ depend on whether or not the $j=7/2$ states are taken into account in the ground state. As a result, if the $j=7/2$ states are disregarded, the XMCD intensity increases by about 30%, although the branching ratio is almost unchanged. This explains the difference in the XMCD intensities in Figs. 5 and 7 (with $U_{ff}=\infty$), where the final-state mixing effect does not change the XMCD spectra. In the weakly mixed-valence case, the calculations by disregarding the $j=7/2$ states can provide us with a meaningful result as an approximation method, but it should be noted that the result of the XMCD spectrum is not sufficiently exact but requires some corrections in the intensity. If the value of V_g increases (decreases), the correction becomes larger (smaller).

VII. CONCLUDING REMARKS

We have presented a unified theory of XMCD at the $L_{2,3}$ edges of mixed-valence Ce compounds by taking into account all of the important ingredients: the hybridization between Ce $4f$ and ligand states, the magnetic polarization of Ce $4f$ states, the exchange interaction between Ce $5d$ and $4f$ states, and the spin polarization of Ce $5d$ states due to the hybridization with the spin-polarized ligand band. The theory has been applied to the calculations of XAS and XMCD spectra for a series of Ce compounds: the localized Ce^{3+} system, and the weakly and strongly mixed-valence Ce systems. The results agree satisfactorily with the experimental ones for ferromagnetic systems, $CeRu_2Ge_2$ and $CeFe_2$, and a paramagnetic system $CePd_3$ under an external magnetic field.

In the initial part of our calculations, some simplifying assumptions were made. We disregarded the hybridization between the Ce $4f$ and ligand states in the final state and also neglected the contribution from the Ce $4f^2$ configuration by putting $U_{ff}=\infty$. However, we also performed some calculations including these effects and checked the validity of disregarding these effects. At least for the weakly mixed-valence systems with $V_g=0.1$ eV or smaller, it is confirmed that the final-state hybridization and the Ce $4f^2$ contribution can be disregarded.

Throughout the paper, we confined ourselves into a limiting case where the width of the ligand band vanishes. By this assumption, the calculations of XAS and XMCD spectra were much simplified, avoiding a complicated many-body process due to the itinerant nature of the ligand band. In order to make more quantitative calculations to compare precisely with experimental XAS and XMCD data, it would be necessary to take into account a finite width of the ligand band, as well as that of the Ce $5d$ band. Nonetheless, despite this extreme simplicity, our model presented in this paper should be very useful for understanding the qualitative behavior of the XAS and XMCD spectra of a variety of different Ce compounds. It provides a good starting point for sorting out the important physics that will be necessary in order to eventually provide a more quantitative theory for these systems that better handles the itinerant nature of the ligand and Ce $5d$ states. Some calculations of XAS and XMCD spectra, where a finite width of the ligand band is taken into account, are now in progress and will be published in the near future.

In this paper the change in XAS and XMCD spectra is studied by changing the parameter values of V_g, V_f, U_{ff}, and D_{spin}. It is found that by changing V_g, U_{ff}, and D_{spin} the change in XMCD spectrum is much larger than that in XAS (see Figs. 4, 7, and 8). On the other hand, the change in V_f causes the changes larger in XAS than in XMCD (see Fig. 6), in marked contrast to the change in other parameters. The reason for this is that the parameters V_g, U_{ff}, and D_{spin} describes the ground-state character of the system (or both ground-state and final-state characters), whereas V_f describes only the final-state character. Since the XMCD spectrum is the higher-order quantity than the XAS spectrum, a small change in the ground-state character is reflected in XMCD more sensitively than in XAS. The situation is different for the change in the final-state character. It is well known that the integrated intensity of XAS and XMCD spectra is determined only by the ground-state character, independent of the final-state character. As seen from Fig. 6, the integrated intensity of XAS and XMCD is almost conserved in each of L_2 and L_3 edges with the change in V_f. Since the XAS spectra at L_2 and L_3 edges have double-peak structure, a change in V_f causes the oscillator strength to be transferred from the higher-energy peak to the lower-energy peak with the integrated intensity kept constant. On the other hand, the XMCD spectrum has a single-peak structure so that no transfer of oscillator strength occurs, and thus the change in the XMCD spectrum with changing V_f is much smaller than in the XAS spectrum. This is an interesting fact which is related with the sum rule of XAS and XMCD, and a more quantitative understanding will be left in future investigations.

Finally, we would like to point out that the theoretical framework presented in this paper can also be applied in describing the XMCD spectra of mixed-valence Yb compounds and that it will be very interesting to calculate the XMCD spectra of mixed-valence Ce and Yb compounds in extremely high magnetic field. Such calculations are now in progress[20] and will be published in the near future.

ACKNOWLEDGMENT

The present author would like to thank T. Koide for carefully reading the paper and for giving useful comments.

*Also at RIKEN Harima Institute, 1-1-1 Kouto, Sayo, Hyogo 679-5148, Japan; akio_kotani_jp@yahoo.co.jp

[1] C. M. Varma, Rev. Mod. Phys. **48**, 219 (1976).
[2] See, for instance, *Valence Fluctuations in Solids*, edited by L. M. Falicov, W. Henke, and M. B. Maple (North-Holland, Amsterdam, 1981).
[3] O. Gunnarsson and K. Schönhammer, Phys. Rev. B **28**, 4315 (1983).
[4] See, for instance, F. M. F. de Groot and A. Kotani, *Core Level Spectroscopy of Solids* (CRC, Boca Raton, FL/Taylor & Francis, London, 2008).
[5] J. C. Parlebas, K. Asakura, A. Fujiwara, I. Harada, and A. Kotani, Phys. Rep. **431**, 1 (2006).
[6] C. Giorgetti, S. Pizzini, E. Dartyge, A. Fontaine, F. Baudelet, C. Brouder, Ph. Bauer, G. Krill, S. Miraglia, D. Fruchart, and J. P. Kappler, Phys. Rev. B **48**, 12732 (1993).
[7] F. Baudelet, Ch. Giorgetti, S. Pizzini, Ch. Brouder, E. Dartyge, A. Fontaine, J. P. Kappler, and G. Krill, J. Electron Spectrosc. Relat. Phenom. **62**, 153 (1993).
[8] J. P. Kappler, A. Herr, G. Schmerber, A. Derory, J. C. Parlebas, N. Jaouen, F. Wilhelm, and A. Rogalev, Eur. Phys. J. B **37**, 163 (2004).
[9] J. Ph. Schillé, I. Poinsot, C. Giorgetti, P. Sainctavit, G. Fischer, C. Brouder, F. Bertran, M. Fiazzi, C. Godart, E. Dartyge, J. P. Kappler, and G. Krill, Physica B **199-200**, 563 (1994).
[10] K. Fukui, H. Matsuyama, I. Harada, J. C. Parlebas, and A. Kotani, J. Electron Spectrosc. Relat. Phenom. **104**, 67 (1999).
[11] H. Matsuyama, I. Harada, and A. Kotani, J. Phys. Soc. Jpn. **66**, 337 (1997).
[12] M. van Veenendaal, J. B. Goedkoop, and B. T. Thole, Phys. Rev. Lett. **78**, 1162 (1997).
[13] K. Asakura, K. Fukui, H. Ogasawara, I. Harada, J. C. Parlebas, and A. Kotani, J. Phys. Soc. Jpn. **73**, 2008 (2004).
[14] A. Kotani, J. Phys. Soc. Jpn. **77**, 013706 (2008).
[15] A. Kotani, T. Jo, and J. C. Parlebas, Adv. Phys. **37**, 37 (1988).
[16] T. Jo and S. Imada, J. Phys. Soc. Jpn. **62**, 3721 (1993).
[17] The expression of Eq. (6) is slightly different from the exchange energy by Jo and Imada (Ref. 16) and by Matsuyama *et al.* (Ref. 11) because they used the *LS* coupling scheme for the Ce $4f$ states but we use the *JJ* coupling scheme. In describing the Ce $4f$ states, the *JJ* scheme is better than the *LS* scheme due to the strong spin-orbit coupling, but the effect of the exchange energy on the XMCD spectrum is not seriously different in the two schemes.
[18] The factor $[1-\alpha E_{\mathrm{ex}}(m_d,s_d;j,j_z)]$ in Eq. (9) of Ref. 14 is a misprint for $[1-\alpha E_{\mathrm{ex}}(m_d,s_d;j,j_z)]^{1/2}$.
[19] To be more exact, the function $f_{j',j,j_z}(\omega)$ includes the ground-state energy E_g, which depends on the mixed-valence character of the ground state. However, E_g causes only a shift of $f_{j',j,j_z}(\omega)$ and gives no influence on the spectral shape and intensity.
[20] A. Kotani, presented at 21st International Conference on X-Ray and Inner-Shell Processes, 2008 [Eur. Phys. J. Spec. Top. (to be published)].